

Energy Loss of Particles in Pulsar Radio Emission Region

H.G. Wang, Y. Wang, G.J. Qiao, R.X. Xu

CAS-PKU joint Beijing Astrophysical Center and Department of Astronomy,
Peking University, Beijing 100871, China

Received _____; accepted _____

ABSTRACT

Extremely relativistic particles play an important role in various radiative mechanisms of pulsar radio as well as high-energy emission. It is thus very essential to estimate the Lorentz factor of these particles in the radiation regions both observationally and theoretically. In this paper, according to the frequency dependence of component separation and considering some radiation processes, we obtain the Lorentz factor and its variation in the radiation region observationally for seven multi-frequency observed pulsars. It is found that the Lorentz factor decays substantially in the emission region, and the decay can not be well understood by all known energy loss processes. This result hints that there are some unknown processes which are responsible to loosing energy effectively.

Subject headings: Pulsars - Radiation mechanisms

1. Introduction

The energy loss of relativistic particles in pulsar magnetosphere have been studied by many authors (Daugherty & Harding 1989, Sturner 1995, Zhang et al. 1997, Lyubarskii & Petrova 2000, hereafter LP2000). Three possible energy loss mechanisms, i.e., inverse Compton scattering (ICS) of thermal photons by relativistic particles, triplet pair production and curvature radiation of particles, were investigated by Sturner (1995). It is found that the resonant ICS process in strong magnetic fields is the dominant energy loss mechanism when the Lorentz factors are between 10 and 10^4 and pulsar surface temperature is $\sim 10^6$ K. Considering resonant ICS of thermal photons by secondary particles ($10 < \gamma < 10^4$) above the pulsar inner gap, LP2000 found that the ratio of Lorentz factor to its initial value, γ/γ_0 , decreases generally to 40% within a height $\lesssim 10$ km along the magnetic field lines above the polar cap and nearly keeps constant at higher distances.

The Lorentz factor γ can be estimated from some observational properties (e.g. microstructure width) of pulsars. Lange et al. (1998) assumed that the widths of microstructure are related to the beam widths of relativistic particles. They found that the derived γ , according to the observed micropulse typical widths of PSR B0950+08, PSR B1133+16 and PSR B2016+28, is in a range from 240 to 520 if the angle between the line of sight and pulsar rotation axis is 90° . γ could be even larger since this angle may be less than 90° (Lyne & Manchester 1988, hereafter LM88, Rankin 1993).

However, as far as we know, there are few works trying to derive energy loss of particles in the emission region observationally. Thorsett (1991, hereafter T91) studied the dependence of component separation on observing frequency for seven pulsars. It is found that the separation of emission components varies

with observing frequencies smoothly. According to this observational analysis and employing pulsar radio emission models, we calculate the γ factors at different heights. It is found that in the radio emission region, the Lorentz factor decays significantly, which can not be understood by the energy loss processes known hitherto.

In §2 the observational facts of the frequency dependence of component separation are introduced. The basic assumption, calculation and results are showed in §3. In §4, conclusions and discussions are presented.

2. The frequency dependence of component separation

It is based on the dependence of component separation $\Delta\theta$ on observing frequencies ν to find out the energy distribution of particles in the emission region of pulsars. The dependence has been studied for a long time. Earlier analysis found that a simple power law could not fit the frequency dependence of component separation (hereafter FDCS) for most pulsars (Lyne et al. 1971, Sieber et al. 1975, Rankin 1983, Slee et al. 1987). Traditionally two power laws were introduced,

$$\Delta\theta = \begin{cases} A_1\nu^{-\alpha_1}, & (\nu < \nu_b), \\ A_2\nu^{-\alpha_2}, & (\nu > \nu_b), \end{cases} \quad (1)$$

where the break frequency ν_b is usually between 0.14–1.5GHz, $\alpha_2 < \alpha_1$ indicating that at higher frequencies the component separation is less frequency dependent. Rankin (1983) even introduced a third power-law at intermediate frequency to fit PSR B1133+16. Collecting all available data, T91 restudied the FDCS for seven pulsars that exhibit double- or multiple-component average profiles, and proposed a smooth function,

$$\Delta\theta = A\nu^{-n} + \Delta\theta_{\min}, \quad (2)$$

to model for each pulsar (for multiple-component profiles, the component separation is the width between the two peaks of outmost cone). As T91 pointed out, it was mainly the insufficient sampling that led those earlier works to report a break frequency. Similar to the FDCS, the average profile width measured at 50% or 10% of component peaks also narrows as frequency increases (Rankin 1983, Xilouris et al. 1996).

Our following analysis and results are based on Eq.(2). On the one hand, the index n and minimum component separation $\Delta\theta_{\min}$ were given by T91. On the other hand, $\Delta\theta$ is a geometrical result which depends on emission height, and ν is model-dependently related to the Lorentz factor in the emission region. Combining these two hands, we can derive a relationship between the distances and the Lorentz factors, when the geometric effect and a radio emission model are involved.

3. Results: Electron Lorentz factor and emission distance

Two assumptions are used in our analysis: 1) the magnetic field lines are dominantly dipolar in pulsar radio emission region, 2) radio emission arises from the last open field lines. The beaming angle θ_μ (the angle between the tangent of magnetic field and the magnetic axis) can then be calculated from the viewing geometry (LM88),

$$\sin^2\left(\frac{\theta_\mu}{2}\right) = \sin^2\left(\frac{\Delta\theta}{4}\right) \sin\alpha \sin(\alpha + \zeta) + \sin^2\left(\frac{\zeta}{2}\right), \quad (3)$$

where the impact angle ζ is the angle between the line of sight and magnetic axis, α is the inclination angle. α and ζ can be obtained from observations (LM88, Rankin 1993). Geometrically, one has the following equations (Qiao & Lin 1998, hereafter QL98) about θ_μ , from which the distance r can be calculated,

$$\tan\theta_\mu = \frac{3 \sin\theta \cos\theta}{(2 - \sin^2\theta)}, \quad (4)$$

$$\sin^2 \theta = \frac{r}{R_{\text{LC}}}, \quad (5)$$

where the polar angle θ is the angle between position vector \mathbf{r} (from neutron star center to emission point) and the magnetic axis, $r = |\mathbf{r}|$, $R_{\text{LC}} = \frac{cP}{2\pi}$ is the radius of light cylinder, with c the light velocity and P the pulsar rotating period.

The Lorentz factor γ of relativistic particles can be model-dependently obtained for a given r . Among pulsar radio emission models, the curvature radiation model (e.g., Ruderman & Sutherland 1975, hereafter RS75) and the ICS model (Qiao 1988, QL98) predict different functions of $\nu = \nu(\gamma, r)$, which will be used below to calculate $\gamma = \gamma(r)$, respectively.

In the RS75 model, relativistic particles give out emission through curvature radiation with frequency

$$\nu = \frac{3}{2} \gamma_{\text{CR}}^3 \left(\frac{c}{2\pi\rho} \right), \quad (6)$$

then,

$$\gamma_{\text{CR}} = \left(\frac{4\pi\rho\nu}{3c} \right)^{1/3}, \quad (7)$$

where ‘CR’ denotes ‘curvature radiation’, ρ is the curvature radius at a given point, which reads

$$\rho = \frac{(1 + 3\cos^2 \theta)^{3/2} \sin \theta}{3(1 + \cos^2 \theta)R_{\text{LC}}}. \quad (8)$$

In the ICS model, low frequency electromagnetic wave, with frequency of $\nu_0 \sim 10^6 \text{ Hz}$, is produced by inner gap sparking (though the frequency may vary for different pulsars due to different gap parameters, it does not change the results essentially for a given pulsar, so we simply take the frequency as $\nu_0 \sim 10^6 \text{ Hz}$). These low-frequency photons are up-scattered by relativistic electrons to higher frequencies (QL98),

$$\nu = \frac{3}{2} \gamma_{\text{ICS}}^2 \nu_0 (1 - \beta \cos \theta_i), \quad (9)$$

then one has

$$\gamma_{\text{ICS}} = \left(\frac{2\nu}{3\nu_0} \right)^{1/2} \left(\frac{1}{1 - \beta \cos \theta_i} \right)^{1/2} \quad (10)$$

where $\beta = (1 - 1/\gamma_{\text{ICS}}^2)^{1/2}$, the incident angle θ_i is the angle between the wave vector of low frequency wave and the direction of electron moving along field lines, which can be calculated to be (QL98),

$$\cos \theta_i = \frac{2 \cos \theta + (R/r)(1 - 3 \cos^2 \theta)}{\sqrt{(1 + 3 \cos^2 \theta)[1 - 2(R/r) \cos \theta + (R/r)^2]}}. \quad (11)$$

Employing the observational parameters listed in column 2 to 7 in Table 1, viz., the frequency range, A , n , and $\Delta\theta_{\text{min}}$ given by T91, α and ζ given by LM88, we calculate γ and r numerically and present the data in Fig. 1 for each pulsar. The values of minimum distance r_{min} , maximum Lorentz factors $\gamma_{\text{CR,max}}$ and $\gamma_{\text{CR,min}}$, and the ratio of $\frac{r_{\text{max}}}{r_{\text{min}}}$, $\frac{\gamma_{\text{CR,min}}}{\gamma_{\text{CR,max}}}$ and $\frac{\gamma_{\text{ICS,min}}}{\gamma_{\text{ICS,max}}}$ are listed in table 1, where r_{min} and $\gamma_{\text{CR,max}}(\gamma_{\text{ICS,max}})$ are obtained from the maximum observable frequency, while r_{max} and $\gamma_{\text{CR,min}}(\gamma_{\text{ICS,min}})$ are from the minimum observable frequency.

4. Conclusions and discussions

According to the frequency dependence of component separation of seven pulsars (T91), we obtain a model-dependent relationship between the Lorentz factors γ of extremely relativistic particles and the emission distances r for each pulsar. From the analysis, we have following two points.

- 1). The radio emission of outmost cone typically arise from the distance of about 100km to about 300km, which is consistent with the previous results for these pulsars (e.g. Phillips 1992, Hoensbroech & Xilouris 1997).
- 2). Either γ_{CR} or γ_{ICS} decreases monotonically as r increases. Within the range of r , γ_{CR} may reduce by about 60% and 90 % with respect to their maximum values, respectively. The results reflect that particles undergo severe energy loss

in the radio emission region, which is essentially inconsistent with the theoretical prediction made by many authors, for example, LP2000, as will be discussed below.

Some discussions related to our analysis are as follows.

1). In our analysis, emission is produced at the last open field lines. In fact, to derive $\gamma(r)$, one can also assume that radio emission arises from inner magnetic fields, and the results are nearly the same, for an example, with the radius $R_e = \lambda R_{LC}$, where the factor $\lambda > 1$ (this means that the field lines are closer to the magnetic axis, see QL98). Fig. 2 compares the curves of $\gamma(r)$ obtained for the last open field lines and inner field lines with $\lambda = 1.2$ (corresponds to the field lines satisfying $\theta = 0.91\theta_P$, where θ_P is the polar cap angle defined by the last open field line at pulsar surface) for PSR B 0525+21, from which one can see that the $\gamma(r)$ does not show significant difference. The uncertainty of inclination angle α and impact angle ζ may influence the $\gamma(r)$, as shown in Fig. 3, which presents the $\gamma(r)$ curves for three groups of α and ζ , i.e., $(23.2^\circ, 0.7^\circ)$ (given by LM88), $(23.2^\circ, 2.0^\circ)$ and $(90^\circ, 0.7^\circ)$. Here It shows that the uncertainty of α may change the results of r greatly, but in general, $\gamma(r)$ does not change essentially.

2). Interestingly, our results show that there must be some additional energy-loss processes in the radio emission regions. But so far we did not find any reasonable effective mechanism for the energy loss. Theoretical study, e.g., LP2000, shows that γ nearly does not decay at the emission region higher than 10km if only electron ICS process of the thermal photons from neutron star surface is included. Also pulsar radio emission can not lead electrons loose energy significantly (Lin 1997).

A possible effective process may be the resonant ICS of soft X-rays produced in outer gap with the relativistic particles. Cheng & Zhang (1999) present a model of multi-component X-ray emission from the rotation-powered pulsars, in which

hard thermal and soft thermal X-rays originate from the back-flow current of the outer gap. The directions of the soft X-rays are diffused, so that the resonant ICS may be effective due to proper incident angles. However, there is a criterion to determine whether a pulsar has an outer gap or not (Zhang & Cheng 1997, Cheng & Zhang 1999). The size of the outer gap, which is the ratio between the potential drop of the outer gap and the total potential of the open field lines, limited by the soft thermal X-rays from the pulsar surface, can be determined as,

$$f = 5.5P^{26/21}B_{12}^{-4/7}, \quad (12)$$

where P is the rotation period of pulsars in seconds, B_{12} the surface magnetic field strength in 10^{12} G. Only when $f \leq 1$ can the outer gap exist. Unluckily, we find $f > 1$ for all the seven pulsars, as presented in Table 2, and the outer gap may not exist. It seems that the criterion of Zhang & Cheng needs to be re-investigated, or other energy loss processes should be proposed.

3). It should be emphasized that our result is model dependent. According to other radio emission models, e.g., relativistic plasma emission models (Melrose & Gedalin 1999 and references therein), some other interesting constraints on the relativistic particles or plasma may be obtained. But in this paper we just concentrate on the particle Lorentz factor so that only the Curvature radiation model and ICS model are employed.

We are grateful to Dr. B. Zhang, Dr. J.L. Han and other members of the pulsar group for helpful discussion. This work is partly supported by NSF of China, the Climbing project, the National Key Basic Research Science Foundation of China, and the Research Fund for the Doctoral Program Higher Education.

REFERENCES

- Cheng, K.S. & Zhang, L., 1999, ApJ, 515, 337
- Daugherty, J.K. & Harding A.K., 1989, ApJ, 336, 861
- Hoensbroech, A.von & Xilouris, K.M., 1997,A&A, 324, 981
- Lange, Ch., Kramer, M., Wielebinski, R. & Jessner, A., 1998, A&A,332,111
- Lin, W.P., Thesis of master degree, Peking University
- Lyne, A.G.& Manchester, R.N., 1988, MNRAS, 234, 477
- Lyne, A.G., Smith, F.G. & Graham, D.A., 1971, MNRAS, 153,337
- Lyubarskii, Y.E. & Petrova, S.A., 2000, A&A,355,406
- Melrose, D.B. & Gedalin, M.E., 1999, ApJ,521, 351
- Phillips, J.A., 1992, ApJ,385, 282
- Qiao, G.J., 1988a, Vistas in Astronomy, 31, 393
- Qiao, G.J. & Lin, W.P.,1998, A&A, 333,172
- Rankin, J.M., 1983, ApJ, 274,359
- Rankin,J.M.,1993,ApJSS,85,145
- Ruderman, M.A. & Sutherland, P.G., 1975, ApJ, 196, 51
- Sieber, W., Reinecke, R. & Wielebinski, R., 1975, ApJ, 196,51
- Slee, O.B., Bobra, A.D. & Alurkar, S.K., 1987, Australian J. Phys., 40, 557
- Sturner, S.J., 1995, ApJ, 446,292
- Thorsett, S.E., 1991, ApJ, 377, 263
- Xilouris,K.M., Kramer, M., Jessner, A. et al.,1996, A&A, 309,481
- Zhang, B., Qiao, G.J. & Han, J.L., 1997, ApJ, 491,891

Zhang, L. & Cheng, K.S., 1997, ApJ, 487, 370

Table 1: Parameters given by T91 and our results

PSR B	Freq. Range	A	$\Delta\theta_{\min}$	n	α	ζ	r_{\min}	$\gamma_{\text{CR,max}}$	$\gamma_{\text{ICS,max}}$	$\frac{r_{\max}}{r_{\min}}$	$\frac{\gamma_{\text{CR,min}}}{\gamma_{\text{CR,max}}}$	$\frac{\gamma_{\text{ICS,min}}}{\gamma_{\text{ICS,max}}}$
	(GHz)		(°)		(°)	(°)	(km)					
0301+19	0.1-2.7	86	0.9	0.34	31.9	1.8	59	463	3763	4.4	0.43	0.092
0329+54	0.1-10.7	1059	19.8	0.96	30.8	2.9	169	781	2957	2.2	0.24	0.068
0525+21	0.05-4.9	90	9.5	0.47	23.2	0.7	132	762	6105	4.2	0.28	0.048
1133+16	0.026-10.7	53	4.4	0.50	51.3	3.7	135	819	4062	2.8	0.16	0.031
1237+25	0.08-4.9	79	7.9	0.52	48.2	0.9	106	621	3419	3.1	0.31	0.076
2020+28	0.1-14.8	1103	9.1	1.08	71.2	3.6	71	666	2374	2.3	0.22	0.063
2045-16	0.08-4.9	45	7.9	0.36	36.7	1.1	132	684	4007	2.7	0.30	0.078

Table 2: numerical values of f

PSR B	P (s)	B_{12} (G)	f
0301+19	1.388	1.34	6.98
0329+54	0.715	1.21	3.25
0525+21	3.746	12.25	6.74
1133+16	1.188	2.11	4.44
1237+25	1.382	1.15	7.58
2020+28	0.343	0.81	1.66
2045-16	1.962	4.64	5.27

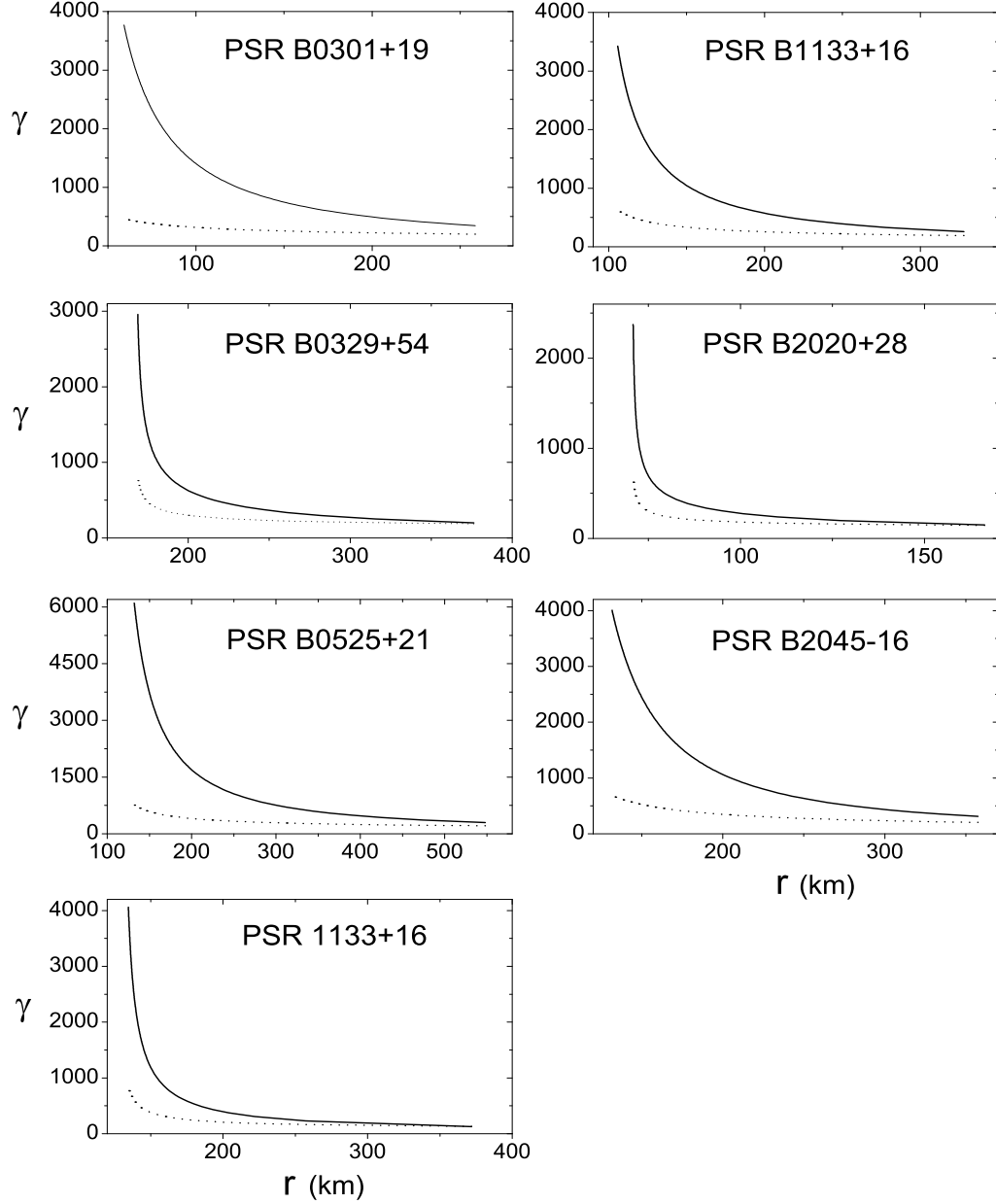


Fig. 1.— The $\gamma(r)$ relationships for seven pulsars. The dot and solid curves represent the data calculated for curvature radiation and inverse Compton scattering respectively.

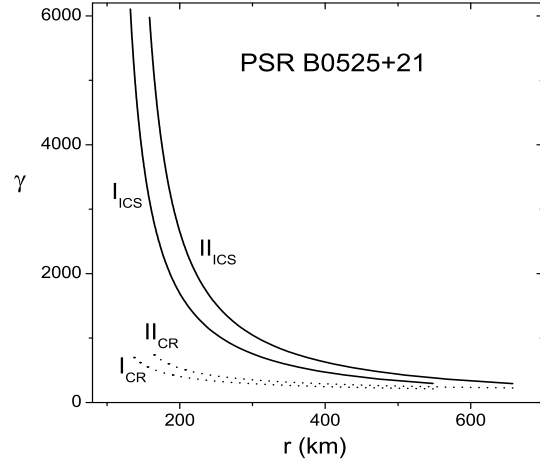


Fig. 2.— The effect of inner field lines to $\gamma(r)$. The curves marked by I are calculated for the last open field lines, and II for the inner field lines with $\lambda = 1.2$. ‘CR’ denotes curvature radiation and ‘ICS’ denotes inverse Compton scattering.

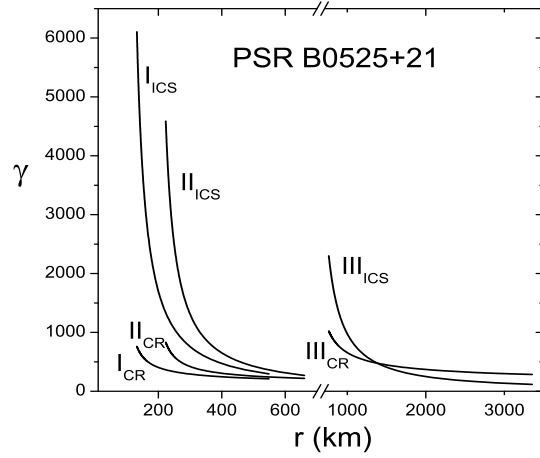


Fig. 3.— The influence of inclination angle α and impact angle ζ to $\gamma(r)$. The curves marked by I are calculated for $(23.2^\circ, 0.7^\circ)$, II for $(23.2^\circ, 2.0^\circ)$ and III $(90^\circ, 0.7^\circ)$. The marks of ‘CR’ and ‘ICS’ are the same as those in Fig.2.